

# June solstice equatorial spread $F$ : On the role of weakening vertical plasma drifts



Weijia Zhan<sup>1</sup>, Fabiano S. Rodrigues<sup>1</sup>, and Marco A. Milla<sup>2</sup>

1. The University of Texas at Dallas, Richardson, TX, USA | 2. The Jicamarca Radio Observatory, Lima, Peru

**Abstract:** We report the results of an experimental and numerical analysis of vertical plasma drifts and unusual equatorial spread  $F$  (ESF) events. The measurements were made using the incoherent scatter radar of Jicamarca Radio Observatory. We found strong evidence of the development of June solstice, post-midnight ESF following the weakening of downward ionospheric drifts. Numerical modeling analysis using SAMI2 provide additional information about the role of weakening vertical drifts in uplifts of the  $F$  layer and stability of the low-latitude  $F$ -region.

## 1. INTRODUCTION

- It is widely believed that pre-reversal enhancement (PRE) of vertical drifts is the main factor for the generation of the generalized Rayleigh-Taylor instability producing ESF events during pre-midnight hours and equinox.
- Much less is known about the source of ESF during June solstice, low solar flux conditions when drifts are generally weak specially during post-midnight hours [e.g. Patra et al., 2009].
- Nicolls et al. (2006) suggested that a weakening downward drift could cause significant  $F$ -region uplifts (apparent increase in  $F$ -region height) and, potentially, destabilize the equatorial  $F$ -region.
- Given the lack of understanding and importance of ionospheric structuring associated with June solstice ESF, this study addresses the following questions: **1. Can we find experimental evidence of weakening downward drifts, uplifts and ESF during June solstice conditions in the American sector?** **2. How does the linear stability of the equatorial  $F$ -region behave during the scenario of a weakening downward plasma drift?**

## 2. METHODOLOGY

- Measurements:** In order to obtain accurate information about equatorial plasma drifts as well as ESF, we used data from the “Drift Mode” experiments of the incoherent scatter radar (ISR) of the Jicamarca Radio Observatory, made between 1994 and 2013. We found observations made in 386 different days; 61 measurements made in June Solstice (June/July) and only 13 (of those 61) were made during low solar flux conditions ( $F_{10.7} \leq 80$  SFU). Post-midnight measurements are severely affected by high sky noise but one night of observations (June 4-5, 2008) was found when geomagnetic conditions were low.
- Ionospheric modeling:** SAMI2 is a physics-based model of the low- and mid-latitude ionosphere (Huba et al., 2000). We modified SAMI2, for this study, to be driven by the vertical drifts measured by the Jicamarca ISR.
- Estimates of  $F$ -region stability:** In order to evaluate the stability of the  $F$ -region we followed the work of Sultan (1996) and computed the linear growth rate of the Generalized Rayleigh-Taylor instability:

$$Y_{RT} = \frac{\sum_p^E}{\sum_p^E + \sum_p^F} \left( V_p - U_L^P - \frac{g_e}{v_{eff}^F} \right) K^F \quad \text{Equation 1}$$

Where:  $\sum_p^E$  and  $\sum_p^F$  are flux-tube integrated E- and F-region Pedersen conductivities, respectively.  $V_p$  is the vertical drift velocity.  $U_L^P$  is the flux-tube integrated neutral wind component perpendicular to the magnetic field and weighted by the Pedersen conductivity.  $g_e$  is local gravity defined;  $v_{eff}^F$  is the flux-tube integrated effective F-region ion-neutral collision frequency.  $K^F$  is defined by  $\frac{1}{N_e} \frac{\partial N_e}{\partial h}$  (where  $N_e$  is the flux tube integrated electron density). The growth rate was computed using SAMI2 outputs.

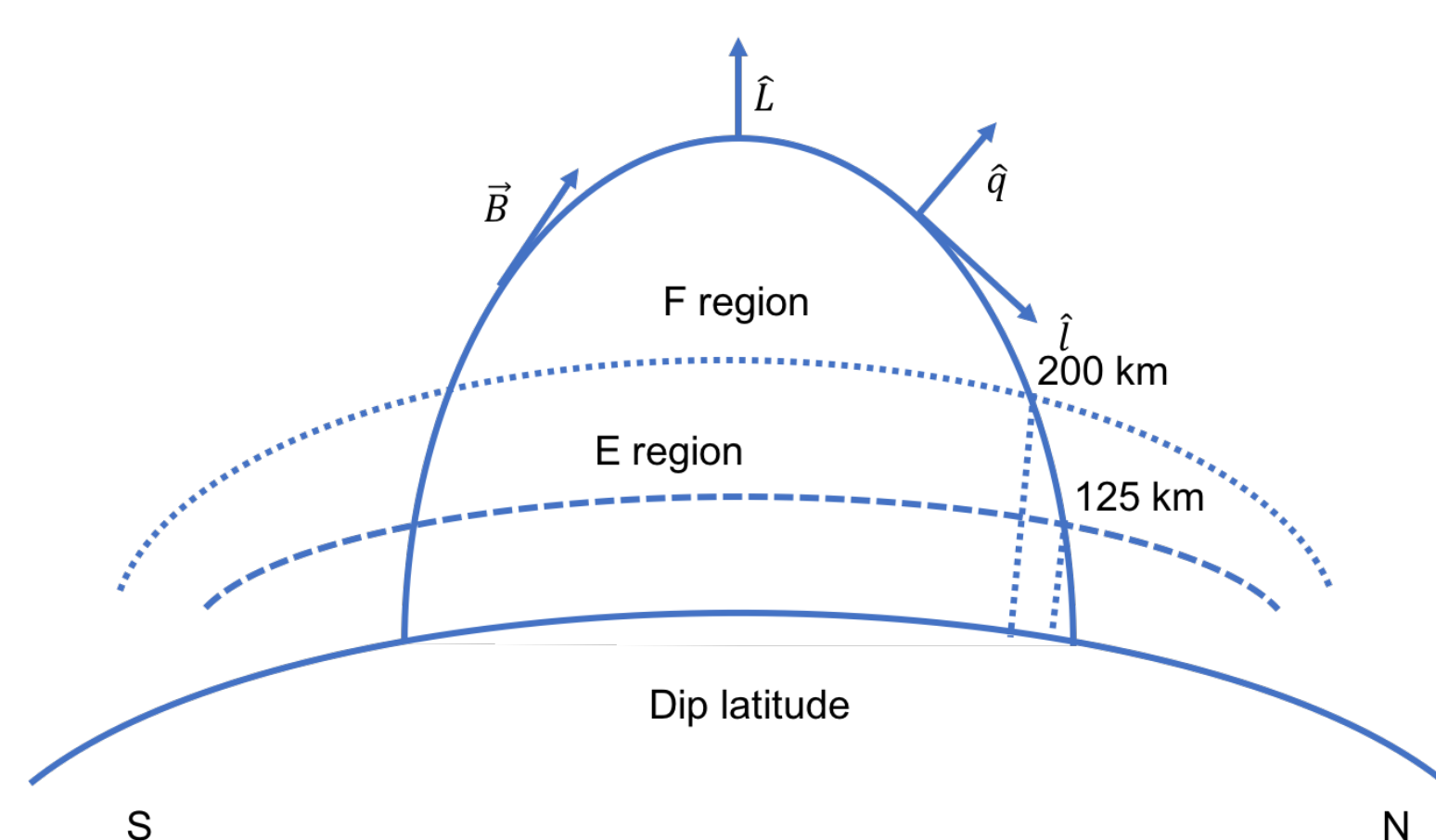


**Figure 1.** Geometry of a dipole magnetic field line.  $\hat{L}$  is the direction of magnetic field,  $\hat{q}$  is the direction of neutral wind perpendicular to magnetic field in meridian plane. Flux tube integration is done from altitude of 125 km in the southern hemisphere along the field line to an altitude of 125 km in the northern hemisphere. The boundary between E and F region is 200 km.

## 3. RESULTS AND DISCUSSION

### 3.1 Jicamarca Measurements: Weakening event of June 4-5, 2008

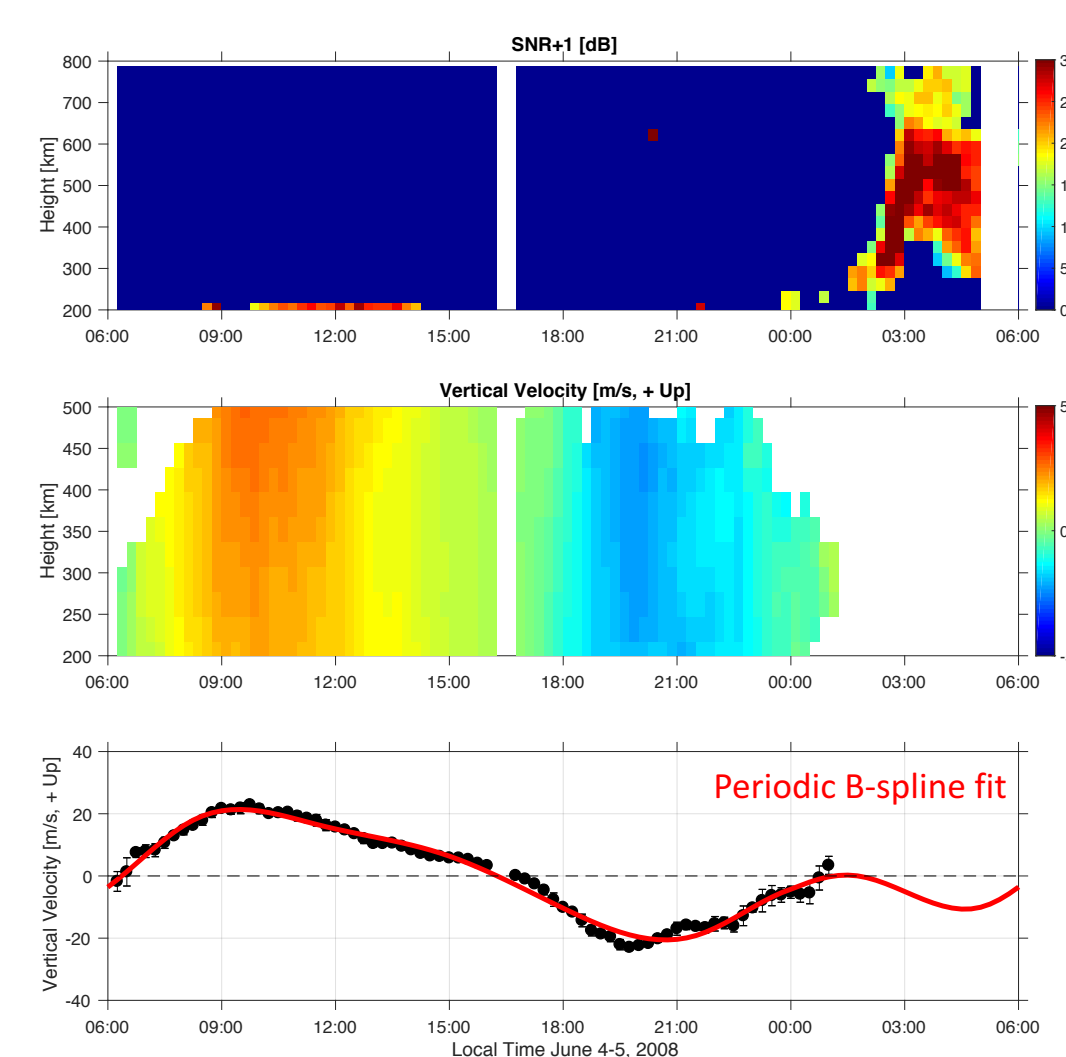


**Figure 2 [Weakening Drifts] Top:** RTI (range-time intensity) map of echoes observed on June 4-5, 2008. ESF event after about 01:00 LT. **Middle:** Altitude versus local time variation of vertical drifts. Weak altitudinal variation. **Bottom:** Local time variation of measured and modelled mean vertical drifts (red solid).

The model drifts were obtained by fitting the measurements with cubic B-splines. Notice the weakening of the drifts prior to ESF development.

**Figure 3 [Uplift] Top:** RTI map of echoes observed on June 4-5, 2008. **Middle:** Local time variation of mean vertical drifts as shown in Figure 2. **Bottom:** Local time variation of the minimum virtual height of the  $F$  layer estimated from digisonde measurements.

An uplift is observed starting around 21:00 LT but more significantly after 00:00 when drifts are very weak.

### 3.2 Simulation of uplift and $F$ -region stability estimates

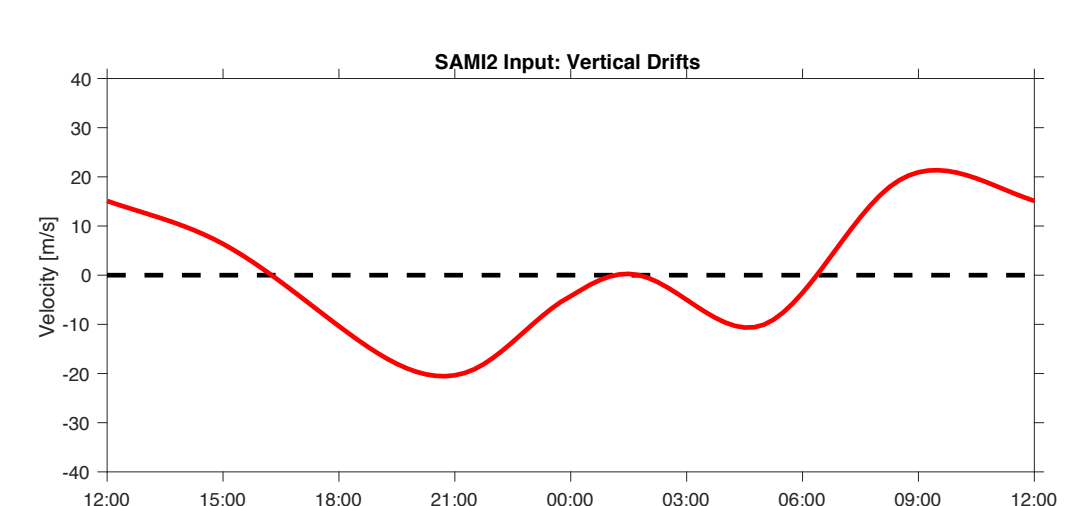


**Figure 4 [Uplift simulation] Top:** local time variation of drifts based on Jicamarca measurements and used to drive SAMI2 simulations. **Bottom:** SAMI2 results showing the altitude versus local time variation of the electron density over Jicamarca.

SAMI2 shows that the  $F$ -region moves upward during the weakening of the downward drifts.

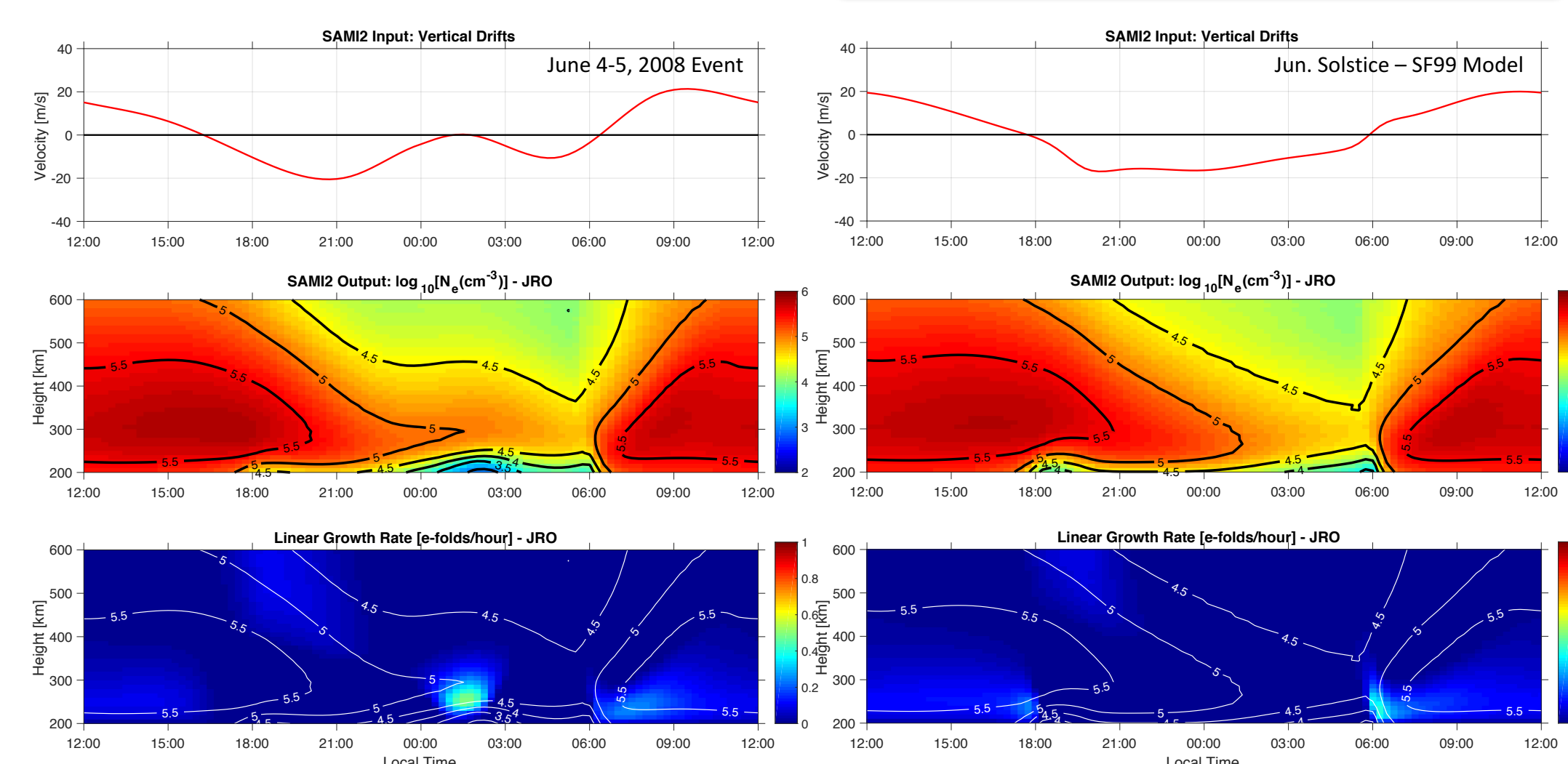


**Figure 5. [Stability] Top panels:** Local time variation of vertical drift observed by the Jicamarca radar (left) and predicted by the Scherliess and Fejer (1999) – SF99 model (right) on June 4-5, 2008. **Middle panels:** SAMI2 outputs of electron density over Jicamarca for the vertical drifts above. **Bottom panels:** Altitude-local time variation of the linear growth rate (Equation 1) estimated from SAMI2 simulations. Note the increased positive growth rate around 01:30 LT on June 5, 2008

### 3.3 Comparisons with December solstice and March equinox

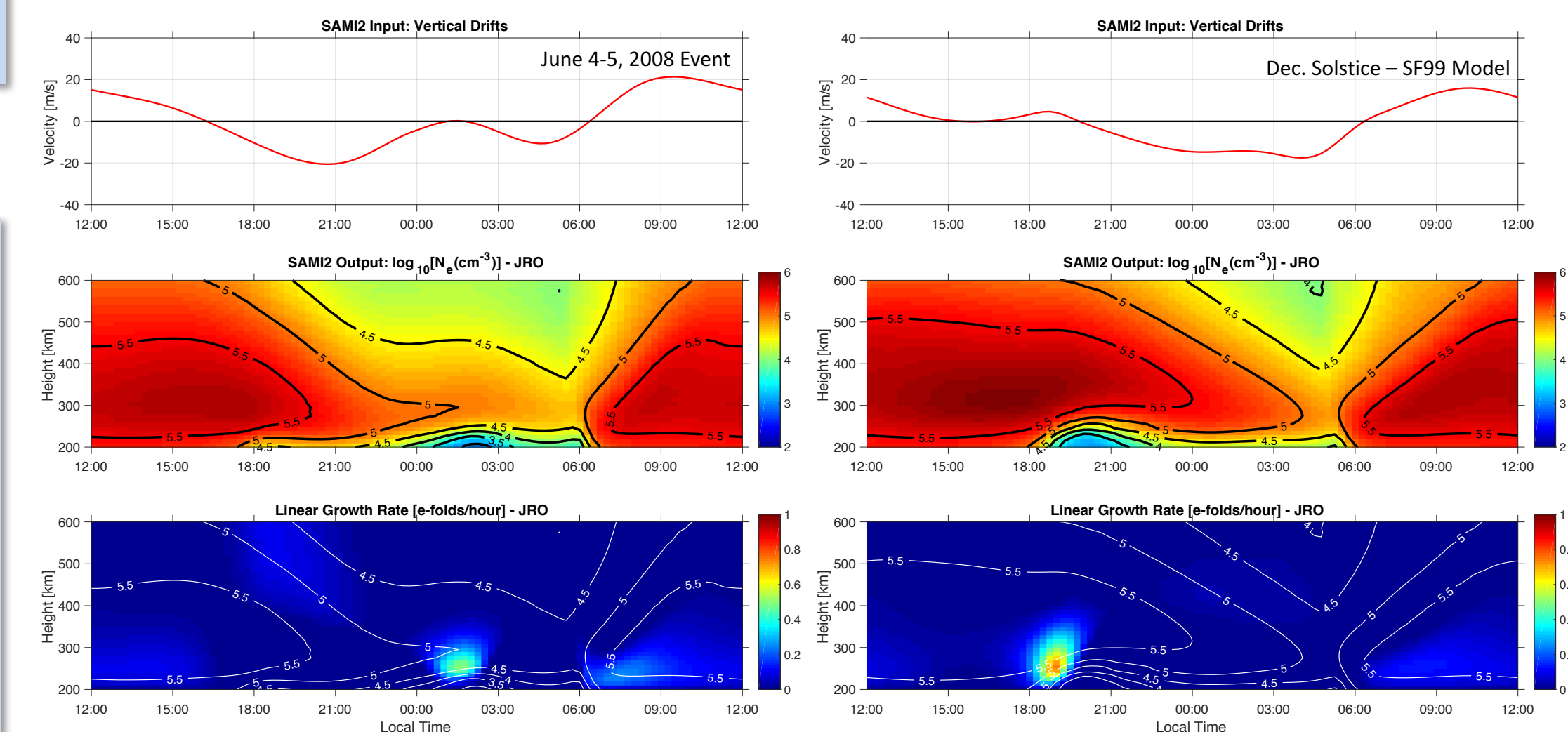


**Figure 6. [Comparison of growth rates]** Same as Figure 5 but now it shows estimates of the growth rate for Dec. solstice (right panels) when ESF is known to occur over Jicamarca in the pre-midnight sector.

The growth rate, as expected, is maximum around PRE hours.

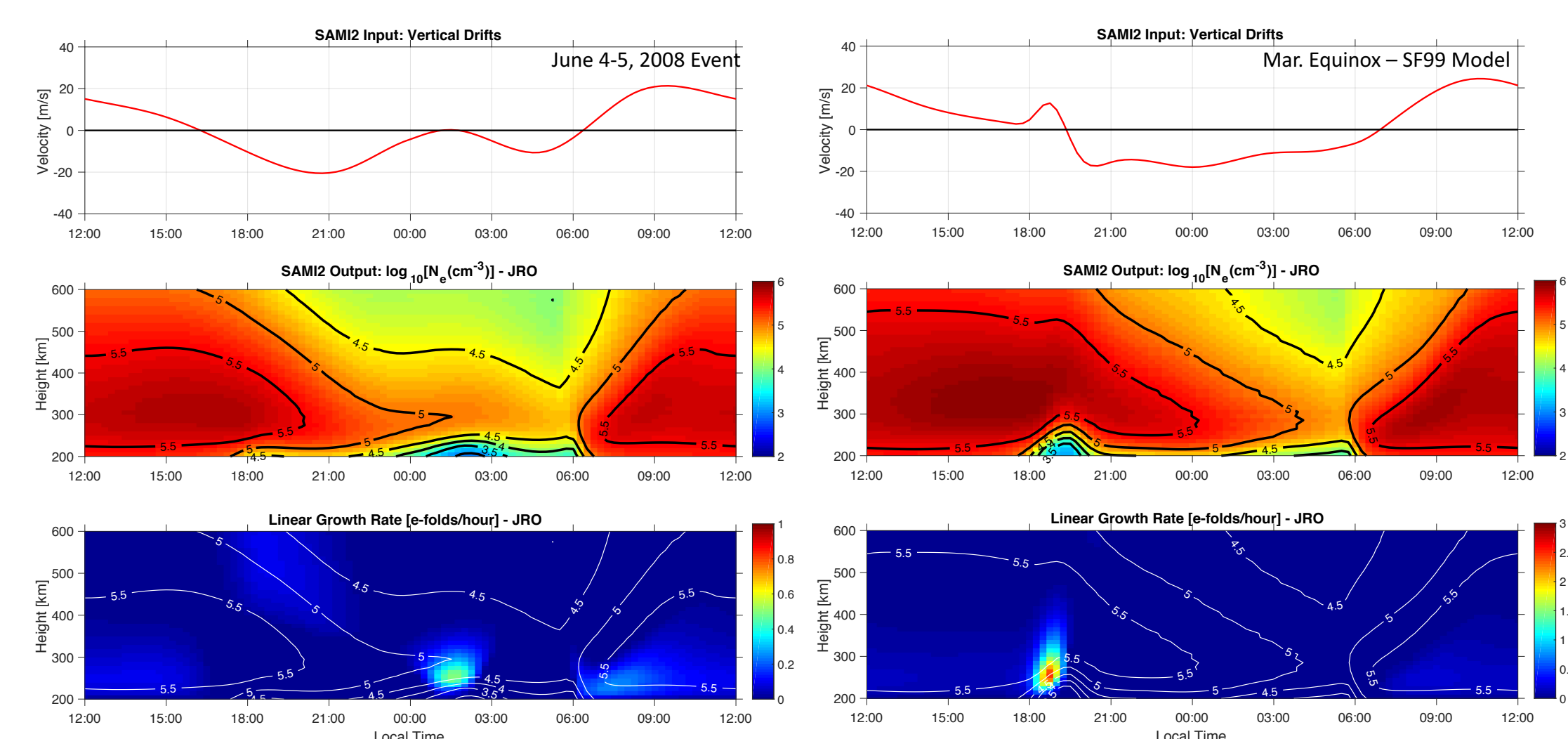


**Figure 7. [Comparison of growth rates]** Same as Figure 5 but now it shows estimates of the growth rate for March equinox (right panels) when ESF is known to occur over Jicamarca in the pre-midnight sector.

The growth rate maximizes, again, around PRE hours and reach values much greater than those obtained for June 4-5, 2008.

## 4. CONCLUSIONS

- We found show strong experimental evidence (based on Jicamarca ISR measurements) that weakening drifts can precede the instability of the equatorial  $F$ -region. This scenario can explain, at least in part, the unexpected occurrence of ESF in the post-midnight sector during June solstice. Recent results of Ajith et al. (2016) point in the same direction.
- SAMI2 simulations, driven by drift measurements, confirm an apparent upward motion of the  $F$ -region during the weakening of the downward drifts.
- Estimates of the linear RT growth rate show that the weakening drifts lead to an unstable equatorial  $F$ -region. The linear growth rates, however, are smaller than those obtained for conditions of typical ESF driven by the PRE. Like in typical ESF, an additional factor is needed to accelerate the development of irregularities.
- Our results also indicate that additional research efforts are needed. These include new, more advanced drift and ESF experiments at Jicamarca during June solstice conditions. Further work testing the accuracy of model outputs will also provide insight on our estimates of the growth rates.

## 5. REFERENCES

- Sultan [1996], J. Geophys. Res., 101, 26875-26891.
- Scherliess and Fejer [1999], J. Geophys. Res., 104(A4), 6829-6842.
- Huba et al. [2000], J. Geophys. Res., 105(A10), 2156-2202.
- Nicolls et al. [2006], Ann. Geophys., 24, 1317-1331.
- Patra et al. [2009], J. Geophys. Res., 114, A12305.
- Ajith et al. [2016], J. Geophys. Res., 121, 9051-9062.